XVIII. NETWORK SYNTHESIS

Prof. E. A. Guillemin	J. Elkan	P. M. Lewis II
Prof. F. M. Reza	E. W. Keller	R. A. Pucel
R. H. Baumann	D. I. Kosowsky	M. Strieby

A. NETWORK SYNTHESIS FOR PRESCRIBED TRANSIENT RESPONSE

This section is a continuation of a discussion, similarly titled, contained in a previous report (1); our objective is to obtain a realizable network system function, h(s), such that the corresponding impulse response approximates some arbitrarily specified time function.

Let us recall the derivation given in the earlier report. Our starting point is the desired network impulse response, f(t), which is shown in Fig. XVIII-1. The duration of this function is denoted by $\tau/2$. A new function, $f_t(t)$, is constructed by repeating f(t) periodically:

$$f_t(t) = f(t) + f(t-\tau) + f(t+\tau) + f(t - 2\tau) + f(t + 2\tau) + \ldots$$

A Fourier series approximation may now be made to $f_t(t)$, and it is convenient to define a function, $f_p(t)$, which is equal to this Fourier series for positive t, and zero for negative t:

$$\begin{aligned} f_p(t) &= \sum_{k=-n}^{n} a_k e^{jk\omega t} && t > 0 \\ &= 0 && t \leqslant 0 \end{aligned} \qquad (1)$$

We next define the functions

$$\begin{aligned} f_1(t) &= \sum_{\substack{k=-n \\ k \text{ even}}}^{n} a_k e^{jk\omega t} && t > 0 \\ &= 0 && t \leqslant 0 \end{aligned} \qquad (2)$$

$$\begin{aligned} f_2(t) &= \sum_{\substack{k=-n \\ k \text{ odd}}}^{n} a_k e^{jk\omega t} && t > 0 \\ &= 0 && t \leqslant 0 \end{aligned} \qquad (3)$$

Their corresponding Laplace transforms are

$$h_1(s) = \mathscr{L}\left[f_1(t)\right] = \sum_{\substack{k=-n \\ k \text{ even}}}^{n} \frac{a_k}{s - jk\omega}$$

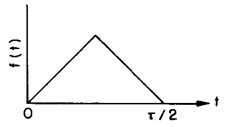

Fig. XVIII-1
The desired network impulse response.

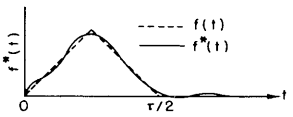

Fig. XVIII-2
The actual and desired network impulse responses.

$$h_2(s) = \mathscr{L}\left[f_2(t)\right] = \sum_{\substack{k=-n \\ k \text{ odd}}}^{n} \frac{a_k}{s - jk\omega}$$

The desired system function may now be written

$$F^*(s) = \frac{4\, h_1 h_2}{h_1 + h_2} \tag{4}$$

which is substantially the same as Eq. 11 of reference 1. Using a star to denote approximation, the impulse response corresponding to Eq. 4 is written $f^*(t)$, and may be found from

$$f^*(t) = \mathscr{L}^{-1}\left(\frac{4\, h_1 h_2}{h_1 + h_2}\right)$$

This function, which is the objective of the synthesis procedure, is shown in Fig. XVIII-2.

$F^*(s)$ should be the desired network system function, but two difficulties arise. First, this function as it stands may not be realizable; that is, it may contain right half plane poles. Second, the initial value of $f^*(t)$ may differ badly from that of f(t). In what follows, we intend to show how these difficulties may be overcome by modifying $F^*(s)$.

With regard to the realizability of $F^*(s)$, the first step is to expand this function in partial fractions. Thereby, we place in evidence any terms involving right half plane poles; these are the troublesome terms in $F^*(s)$, and they are simply subtracted from the partial fraction expansion and thrown away! What is left is, of course, realizable, and is a function of lower degree. It is the desired system function.

One might inquire at this point about the justification for changing $F^*(s)$ in this seemingly arbitrary manner. Briefly, it follows from the expression

$$f^*(t) \approx \mathscr{L}^{-1}\left(\frac{4\, h_1 h_2}{h_1 + h_2}\right) = \mathscr{L}^{-1}\left[F^*(s)\right] \tag{5}$$

which is derived in reference 1. This relation implies that the residues in any right half

plane poles of $F^*(s)$ are small. And, we infer that the right half plane poles may be removed without materially affecting the time function, $f^*(t)$, in the approximating range, which is from 0 to $\tau/2$.

The second difficulty mentioned, that of controlling $f^*(t)$ for small values of t, may be handled by use of the initial value theorem of Laplace transforms. From this theorem, it is not hard to derive

$$f^*(0+) = 4\frac{f_1(0+) \cdot f_2(0+)}{f_1(0+) + f_2(0+)} \tag{6}$$

which relates the initial value of the approximating impulse response to the initial values of $f_1(t)$ and $f_2(t)$. The latter functions derive from a trigonometric polynomial approximation to $f_t(t)$. In our previous discussion, we have referred to the trigonometric polynomial as a Fourier series, but there is no reason why the Fourier coefficients must be used. Accordingly, the coefficients a_k, in Eqs. 1, 2, and 3, may be adjusted if this is desirable; in particular, they are modified to produce any specified value of $f^*(0+)$ whenever such a procedure is motivated by a large discrepancy between $f^*(t)$ and f(t) at small values of t. In this regard, use is made of Eq. 6 in order to postpone actual computation of $F^*(s)$ until after the a_k have been fixed.

The method discussed here has been applied to several problems and seems to be practically promising. Further discussion may be found in a forthcoming technical report and in the references.

M. Strieby

References

1. Quarterly Progress Report, Research Laboratory of Electronics, M.I.T., Jan. 15, 1952, p. 66.

2. M. Strieby, A Fourier method of time-domain synthesis, Proceedings of the Symposium on Modern Network Synthesis, Polytechnic Institute of Brooklyn, April 13-15, 1955.

3. M. Strieby, Time-domain synthesis using trigonometric polynomial methods of approximation, D. Sc. Thesis, Department of Electrical Engineering, M.I.T. (1955).

B. CRYSTAL FILTER DESIGN

A number of techniques have been evolved that greatly simplify the synthesis of bandpass filters employing piezoelectric resonators. Analytical methods of specifying tolerances on crystal units and a device which permits the adjustment of crystal resonators to close tolerances without elaborate equipment have also been developed. The synthesis procedure is essentially based on two types of approximation. The first approximation permits the attenuation, phase, and image impedance characteristics of a bandpass filter to be normalized with respect to bandwidth and center frequency. A single set of

normalized characteristics is sufficient to describe all possible bandpass crystal filters with negligible practical error. The filter "approximation problem" is solved by the addition of normalized characteristics, aided by a graphical method of located attenuation minima. The analytical simplicity afforded by the normalization technique makes possible calculation of all filter losses, including the effects of incidental dissipation, with a minimum of effort. The second approximation is one which permits the element values of the reactances employed in a crystal filter to be calculated in terms of the spacings between the critical frequencies of the reactances. With the aid of this approximation and the normalization already described, the filter synthesis may be accomplished with only a slide rule and a number of simple plotted curves.

The need for this rapid approximate synthesis results from the restrictions imposed on crystal filter characteristics by the crystal itself. In the neighborhood of a mechanical resonant frequency, a piezoelectric vibrator such as a bar or plate cut from a piece of natural quartz, may be replaced by the equivalent circuit shown in Fig. XVIII-3. The crystal "Q," defined as the ratio

$$Q = \frac{2\pi f_a L_1}{R_1} \tag{1}$$

where

$$f_a = \frac{1}{2\pi(L_1 C_1)^{1/2}} = \text{crystal resonant frequency} \tag{2}$$

is generally in the order of 20,000 and may be as high as 500,000, so that R_1 may be neglected for purposes of analysis. The range of electrical parameter values attainable in a piezoelectric crystal is limited by such considerations as resonant frequency, mechanical stability, temperature coefficient, and suppression of spurious modes of vibration. Moreover, a fixed relationship between C_o and C_1 exists in the unmounted resonator by virtue of the electromechanical coupling in the crystal. These restrictions appear in a crystal filter in the form of limitations upon filter bandwidth, image impedance, and in some cases upon the form of attenuation characteristic.

Figure XVIII-4 illustrates the manner in which crystals, inductances, and capacitors may be combined in symmetrical-lattice configurations to yield bandpass-filter characteristics. Curves of series and shunt arm reactances, filter attenuation, and image impedance are sketched as functions of frequency for each filter. Filters 1 and 2 are narrow-band filters, limited by crystal zero-pole spacing (a function of the ratio $r = C_o/C_1$), to bandwidths of less

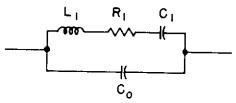

Fig. XVIII-3
Equivalent circuit of crystal resonator.

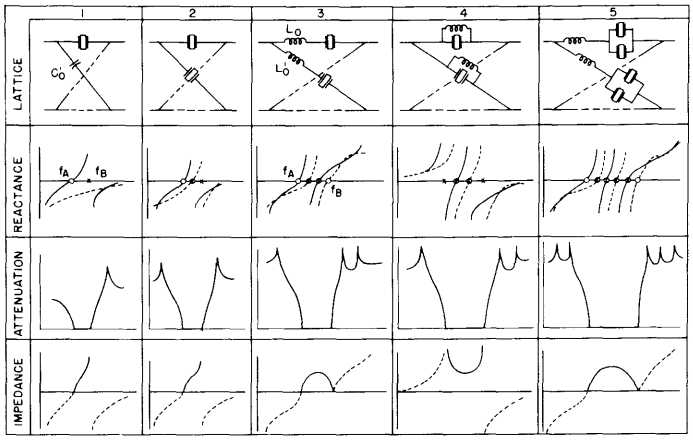

Fig. XVIII-4
Bandpass crystal lattice filters.

than 0.8 per cent of center frequency for quartz. In each of the remaining filters, inductances (L_o, L'_o) have been added in series or in parallel with the crystal elements to widen the filter passband (1). With quartz, bandwidths as large as 13.5 per cent of center frequency are theoretically possible with these combinations.

The simplest bandpass crystal filter (filter 1, Fig. XVIII-4) will be referred to as the "basic" section. The attenuation characteristic of the basic section can have at most one "infinite" peak, the position of which may be placed anywhere outside of the passband by varying the capacitor C'_o. It can be shown (2) that the attenuation characteristic of a filter having n infinite peaks and a bandwidth B is equal to the sum of the characteristics of n basic sections, where each section has a bandwidth B and an attenuation peak corresponding to one of the n peaks of the composite filter. Each filter in Fig. XVIII-4 may therefore be considered equivalent to a number of basic sections (the exact number is one plus the number of passband "coincident" frequencies, designated by ⊗ in Fig. XVIII-4), and only the image impedance depends upon the filter configuration.

The attenuation of the basic section is described (3) by a quantity p given by

$$p = \tanh \frac{\theta}{2} = m^* \left(\frac{f^2 - f_A^2}{f^2 - f_B^2} \right)^{1/2} \qquad (3)$$

where $\theta = \alpha + j\beta$ is the image propagation constant, α is the attenuation constant, β is the phase constant, f_A is the lower cutoff frequency, and f_B is the upper cutoff frequency and

$$m^* = \left(\frac{f_\infty^2 - f_B^2}{f_\infty^2 - f_A^2} \right)^{1/2} \tag{4}$$

where f_∞ is the frequency of the infinite peak.

Equation 3 permits the calculation of all possible attenuation characteristics obtainable with the basic section. Since p is a function of bandwidth and m^* at any frequency, a double infinity of curves would be necessary to cover all possible choices of f_A, f_B, and f_∞. It is possible, however, to find an approximation for p which is independent of bandwidth and center frequency, yet introduces negligible error in practice. The approximate or normalized value of p, denoted by p_o, is given by

$$p_o = m\left(\frac{x+1}{x-1} \right)^{1/2} \tag{5}$$

$$m = \left(\frac{x_\infty - 1}{x_\infty + 1} \right)^{1/2} \tag{6}$$

where

$$x \equiv \frac{f - f_o}{B/2} \tag{7}$$

$$x_\infty \equiv \frac{f_\infty - f_o}{B/2} \tag{8}$$

and

$$f_o = \frac{f_A + f_B}{2} = \text{center frequency} \tag{9}$$

$$B = f_B - f_A = \text{bandwidth} \tag{10}$$

A complete discussion of the derivation of Eqs. 5 and 6 and the errors involved is given in reference 4. A number of normalized basic section characteristics are shown in Fig. XVIII-5. The greatest error in p occurs when the attenuation peak lies at infinity ($x_\infty = \infty$), and when the relative bandwidth ($B_r \equiv B/f_o$) of the filter is large. However, even this error can generally be neglected as the dotted line in Fig. XVIII-5, which shows the exact characteristic for $f_\infty = \infty$ and 10 per cent relative bandwidth, indicates.

To determine the number of basic sections that must be combined to meet a given set of filter specifications, use is made of a series of curves of the function

$$G(x) = \frac{(x_\infty^2 - 1)^{1/2}}{x - x_\infty} \tag{11}$$

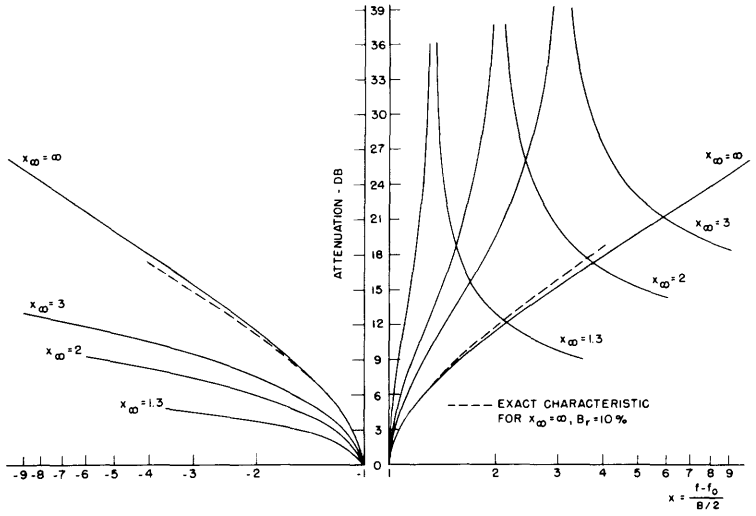

Fig. XVIII-5
Normalized basic section attenuation characteristics.

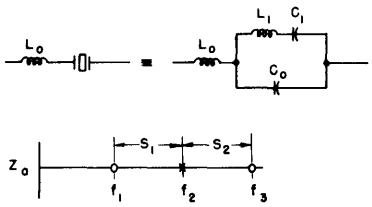

Fig. XVIII-6
Inductance in series with crystal.

for various values of x_∞. These curves are used to determine the frequencies of attenuation minima which result when a number of basic sections are combined (4).

From the graphical addition of the required normalized sections, the number and location of infinite attenuation peaks are determined. The latter information permits the location of the "coincident" frequencies in the filter passband (3, 4). The coincident frequencies, together with the cutoff frequencies completely specify the pole-zero configurations of the lattice series and shunt arm reactances. Finally, the values of the elements making up the lattice reactances are determined, within a multiplying constant (which determines the filter impedance level), from the critical frequencies. On the approximate basis, the required element values are determined in terms of the spacings between the corresponding critical frequencies. For example, consider the combination of an inductance in series with a crystal, which has the zero-pole configuration shown in Fig. XVIII-6. The element values are determined (in terms of C_o) by the crystal resonant frequency f_a, the crystal ratio of capacitances C_o/C_1, and a frequency f_a given by

$$f_a \equiv \frac{1}{2\pi(L_o C_o)^{1/2}} \tag{12}$$

A comparison of the exact and approximate values of f_a, C_o/C_1, and f_a is given below (see App. II of ref. 4).

Quantity	Exact	Approximate
f_a	$\left(f_1^2 + f_3^2 - f_2^2\right)^{1/2}$	$f_2 + (S_2 - S_1)$
f_a	$\frac{f_1 f_3}{f_a}$	$f_2 - \frac{2S_1S_2}{f_2}$
C_o/C_1	$\frac{f_a^2}{f_2^2 - f_a^2}$	$\frac{f_2^2}{4S_1S_2}$

When the reactances are combined in a lattice configuration, the specification of element values by the approximation method is further simplified by determining ratios between corresponding elements in the series and shunt arms of the lattice. These ratios, and the crystal ratios of capacitances (C_o/C_1), which may be calculated by slide rule, are important in determining whether or not the filter is physically realizable in terms of the electrical parameter values obtainable in a crystal resonator.

With the same methods employed in deriving Eqs. 5 and 6, the filter image impedance and phase characteristics may be normalized. From this data, reflection and interaction losses are easily calculated. Still another application of approximation techniques makes possible the analytical determination of tolerances on crystal units, in terms of the corresponding effects upon filter attenuation (4).

A significant problem in the realization of crystal filters has been the procurement of crystal units with characteristics that are held to the close tolerances required for lattice filters. The average crystal grinder does not have the elaborate equipment necessary for making the required measurements (5). However, a device has been developed and tested (see Chap. VI of ref. 4) which permits the adjustment of crystal resonators to very close tolerances with standard laboratory equipment. This device, which is similar in configuration to filter 2 in Fig. XVIII-4, makes use of the high sensitivity of a bridge network to element variations.

The techniques and equipment discussed above have been employed in the design and construction of a number of filters. Because of the low dissipation and high stability of the crystal element, a very close agreement may be expected between the calculated and measured characteristics of a crystal filter. To illustrate this agreement, the insertion loss of a wide-band lattice filter is shown in Fig. XVIII-7. The filter is of the type designated as filter 3 in Fig. XVIII-4, with the series inductances equal ($L_o = L_o'$).

The significant portions of this research will be published in a technical report.

The high selectivity obtainable in filters employing quartz resonators makes such filters very desirable for use in spectrum analysis equipment, carrier communication

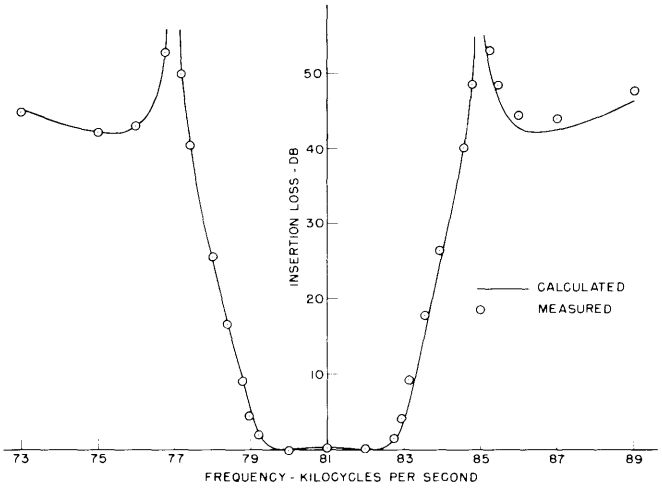

Fig. XVIII-7
Insertion loss characteristic of wideband filter.

systems, single-sideband transmission, and many other applications. As a result of the techniques developed in the course of this research, the availability of economical crystal filters to industry and research laboratories may be substantially increased.

D. I. Kosowsky

References

1. W. P. Mason, Electric wave filters employing quartz crystals as elements, Bell System Tech. J. 13, 405-452 (1934).
2. E. A. Guillemin, Communications Network, Vol. VII (John Wiley and Sons, Inc., New York, 1935), Chap. X.
3. W. P. Mason and R. A. Sykes, Electric wave filters employing quartz crystals with normal and divided electrodes, Bell System Tech. J. 19, 221-248 (1940).
4. D. I. Kosowsky, The synthesis and realization of crystal filters, D. Sc. Thesis, Department of Electrical Engineering, M.I.T. (1955).
5. C. F. Booth, The application and use of quartz crystals in telecommunications, J. Inst. Elec. Engrs. (London) 88, 3, 97-128 (1941).

C. INTERMEDIATE-FREQUENCY AMPLIFIERS

1. Intermediate-Frequency Amplifiers with Linear Phase Characteristics

The most commonly used transfer characteristics of i-f amplifiers are Butterworth (maximally flat amplitude response), Chebyshev (equi-ripple amplitude response), and synchronously-tuned characteristics. To these three categories there is added here a

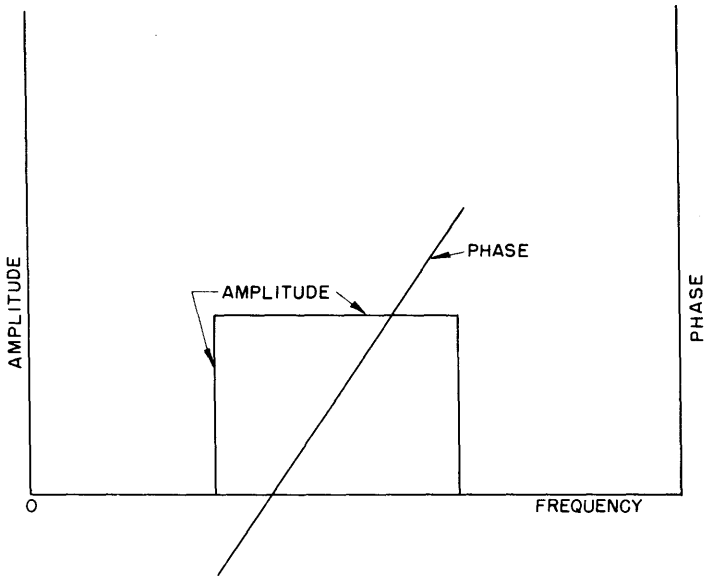

Fig. XVIII-8
Ideal passband.

fourth, termed linear-phase characteristics. All four categories are approximations to the so-called ideal passband. The ideal passband has a rectangular amplitude response of finite width and height and a linear-phase response as shown in Fig. XVIII-8.

Butterworth characteristics optimize the flatness of the passband, Chebyshev characteristics optimize the steepness of the cutoff. Synchronous tuning does not optimize any aspect of the passband, but completely eliminates overshoots in the step-function response. Linear-phase characteristics optimize, in the limited sense defined below, the phase response of the approximation to the ideal passband. Such characteristics are particularly desirable in phase measurement systems and in phase- and frequency-modulation systems.

Since delay (also called group delay or envelope delay) is the derivative of phase with respect to frequency, optimally linear-phase response is equivalent to optimally flat delay. Although there is no unique optimum, it seems sensible to exclude oscillatory approximations to the ideal and consider only single-peaked delay characteristics. The optimum delay characteristic, then, has a maximum number of vanishing derivatives at the peak (band center).

The details of the phase and amplitude response of an i-f amplifier are most easily studied with the help of lowpass prototypes. To obtain a specific bandpass characteristic, the corresponding lowpass prototype characteristic is first designed and then translated to the desired part of the spectrum by a lowpass-bandpass transformation.

The transfer functions of lowpass networks with optimally flat delay have been given

by Thomson (1) and Storch (2). Another derivation is given in reference 3. Such networks are referred to as linear-phase prototypes here. Designating the transfer function of the n^{th} order linear-phase prototype by $H_n(\lambda)$, one has

$$H_n(\lambda) = \frac{a}{\theta_n(\lambda)} \tag{1}$$

where $\theta_n(\lambda)$ is the n^{th} order Bessel polynomial given by

$$\theta_n(\lambda) = \sum_{r=0}^{n} \frac{(n+r)!}{(n-r)!\, r!\, 2^r} \cdot \lambda^{n-r} \tag{2}$$

where $\lambda = \rho + j\nu$ is a complex frequency variable normalized on the reciprocal of the zero-frequency delay, $\nu_o = 1/\tau_o$. If the actual complex frequency is called Λ, one has $\lambda = \Lambda/\nu_o$; "a" is an arbitrary constant. To normalize the magnitude of $H_n(\lambda)$ so that $H_n(0) = 1$, the constant must be taken as $a = (2n - 1)!! \equiv 1 \cdot 3 \cdot 5 \ldots (2n - 1)$.

The properties of linear-phase prototypes of interest in the design of i-f amplifiers are summarized in the following paragraphs. More details will be found in Section 2-C of reference 3.

Table XVIII-1 lists the first few Bessel polynomials and a recurrence formula from which higher-order polynomials can easily be constructed. Table XVIII-2 lists the roots

Table XVIII-1

The Bessel Polynomials

$$\theta_n(\lambda) = \sum_{r=0}^{n} \frac{(n+r)!}{(n-r)!\, r!\, 2^r} \cdot \lambda^{n-r}$$

n	$\theta_n(\lambda)$
1	$\lambda + 1$
2	$\lambda^2 + 3\lambda + 3$
3	$\lambda^3 + 6\lambda^2 + 15\lambda + 15$
4	$\lambda^4 + 10\lambda^3 + 45\lambda^2 + 105\lambda + 105$
5	$\lambda^5 + 15\lambda^4 + 105\lambda^3 + 420\lambda^2 + 945\lambda + 945$

Recurrence Formula

$$\theta_{n+1}(\lambda) = (2n + 1)\, \theta_n(\lambda) + \lambda^2\, \theta_{n-1}(\lambda)$$

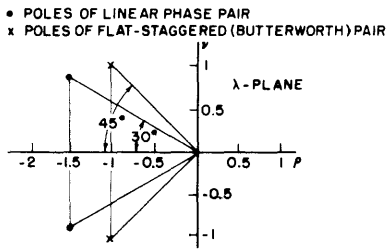

Fig. XVIII-9
Comparison of pole positions.

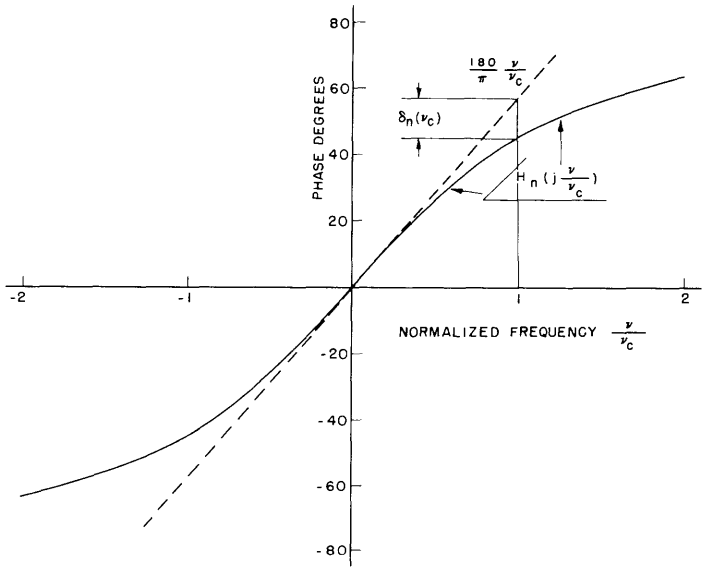

Fig. XVIII-10
Phase deviation from linearity of n^{th} order linear-phase prototype at 3-db cutoff frequency.

of the first nine Bessel polynomials, that is, the poles of the linear-phase prototypes of orders 1-9. There is, in general, no easy geometrical way of obtaining these poles, such as exists for Butterworth and Chebyshev transfer functions. The only exception is the linear-phase pair whose poles lie on radii vectores forming 30° angles with the negative real axis (ρ-axis). The poles of the flat-staggered (Butterworth) pair, by contrast, lie on 45° radii vectores. This is illustrated in Fig. XVIII-9.

Table XVIII-3 lists the deviation from perfect linearity of the phase response at the 3-db cutoff frequency, ν_c, of the linear-phase prototypes, and Fig. XVIII-10 illustrates its use.

A summary of the most frequently used properties of and formulas for linear-phase prototypes follows.

NORMALIZED TRANSFER FUNCTION

$$H_n(\lambda) = \frac{(2n-1)!!}{\sum_{r=0}^{n} \frac{(n+r)!}{(n-r)!\, r!\, 2^r} \cdot \lambda^{n-r}} = \frac{1}{\sum_{k=0}^{n} \frac{2^k \binom{n}{k}}{\binom{2n}{k}} \cdot \frac{\lambda^k}{k!}} \tag{3}$$

$$\lim_{n\to\infty} H_n(\lambda) \to e^{-\lambda} \tag{4}$$

Table XVIII-2*

Poles of Linear-Phase Prototypes $H_n(\lambda)$
Roots of Bessel Polynomials $\theta_n(\lambda)$

n=1	n=2	n=3	n=4	n=5	n=6	n=7	n=8	n=9
-1.0000		- 2.3222		- 3.6467		- 4.9718		- 6.2970
	- 1.5000 ±j0.8660	- 1.8389 ±j1.7544	- 2.8962 ±j0.8672	- 3.3520 ±j1.7427	- 4.2484 ±j0.8675	- 4.7583 ±j1.7393	- 5.5879 ±j0.8676	- 6.1294 ±j1.7378
			- 2.1038 ±j2.6574	- 2.3247 ±j3.5710	- 3.7357 ±j2.6263	- 4.0701 ±j3.5172	- 5.2048 ±j2.6162	- 5.6044 ±j3.4982
					- 2.5159 ±j4.4927	- 2.6857 ±j5.4207	- 4.3683 ±j4.4150	- 4.6384 ±j5.3173
							- 2.8390 ±j6.3539	- 2.9793 ±j7.2915

*To normalize pole constellation on 3-db cutoff frequency, divide all values by $\nu_c = \left[(2n - 1) \ln 2\right]^{1/2}$.

Table XVIII-3

Deviation from Linearity of n^{th} order Linear-Phase Prototype at 3-db Cutoff Frequency

n	Phase Deviation from Linearity $\delta_n(\nu_c)$ Degrees
1	12.3°
2	4.1°
3	1.6°
4	0.4°
5	0.08°
6	0.01°
7	-
8	-

NORMALIZED AMPLITUDE RESPONSE

$$|H_n(j\nu)| = \frac{(2n-1)!!}{\nu^{n+1}\left[(\pi/2\nu)\,J^2_{-n-1/2}(\nu) + (\pi/2\nu)\,J^2_{n+1/2}(\nu)\right]^{1/2}} \tag{5}$$

$$= \frac{(2n-1)!!}{\nu^{n+1}\,D_n(\nu)} \tag{6}$$

$$\approx \exp\left[-\frac{1}{2}\cdot\frac{\nu^2}{2n-1}\right] \tag{7}$$

$$|H_n\left(j\frac{\nu}{\nu_c}\right)| \approx \exp\left[-\frac{1}{2}\left(\frac{\nu}{\nu_c}\right)^2 \ln 2\right] \qquad \text{(independent of n)} \tag{8}$$

The spherical Bessel functions $\left[(\pi/2x)\right]^{1/2} J_{\pm(\mu+1/2)}(x)$ are extensively tabulated in reference 4, and the magnitude of the spherical Hankel functions, $D_\mu(x)$, is less extensively tabulated in reference 5. The gaussian approximation is very close over the passband and good enough about 50 per cent beyond cutoff for $n > 2$, but is not valid outside this range.

PHASE RESPONSE OF $H_n(j\nu)$

$$\phi_n(j\nu) = \nu - \tan^{-1}\frac{J_{n+1/2}(\nu)}{J_{-n-1/2}(\nu)} \tag{9}$$

$$= \nu - \delta_n(\nu) \tag{10}$$

The phase angle of the spherical Hankel functions, $\delta_\mu(x)$, is tabulated (in degrees) in reference 5.

3-DECIBEL CUTOFF FREQUENCY

$$\nu_c \approx \left[(2n-1)\ln 2\right]^{1/2} \tag{11}$$

RELATIVE GAIN-BANDWIDTH FACTOR AND RELATIVE GAIN/RISE TIME RATIO

$$(G \times B) \approx \frac{\left[(2n-1)\ln 2\right]^{1/2}}{\left[(2n-1)!!\right]^{1/n}} \tag{12}$$

$$\lim_{n\to\infty} (G \times B) \to 0 \tag{13}$$

$$\lim_{n\to\infty} \frac{(\dot{G} \times B)_{\text{linear phase}}}{(G \times B)_{\text{synchronous tuning}}} \to \frac{e}{2^{1/2}} \approx 1.91 \tag{14}$$

RISE TIME

$$\tau_r \times \nu_c \approx 2\pi \times 0.34 \qquad \text{(independent of n)} \tag{15}$$

For the bandpass analog, since here the bandwidth B equals twice the cutoff frequency, we have

$$\tau_r \times B \approx 2\pi \times 0.68 \tag{15a}$$

STEP-FUNCTION RESPONSE

$$h_n^{-1}\left(\frac{t}{\tau_o}\right) \approx \frac{1}{\tau_o}\left[\Psi(x) - \frac{1}{4(2n-3)}\,\psi'''(x)\right] \tag{16}$$

where

$$x = (2n-1)^{1/2}\left(\frac{t}{\tau_o} - 1\right) \qquad \text{("standardized" variable)}$$

$$\Psi(x) = \int_{-\infty}^{x} \psi(\xi)\, d\xi$$

$$\psi(x) = \frac{1}{(2\pi)^{1/2}} \exp\left(-\frac{x^2}{2}\right) \qquad \text{(normal or gaussian function)}$$

$$\psi'''(x) = \frac{d^3\psi}{dx^3}$$

n	1	2	3	4
Overshoot (per cent)	0	0.44	0.77	0.85

For large n the overshoot vanishes. The maximum overshoot is less than 2 per cent and occurs in the vicinity of n = 6.

2. Lowpass-Bandpass Transformation

Attention is drawn to the work of Trautman (6). It is shown there that a lowpass prototype with no zeros in the finite λ-plane can be translated into an infinite variety of

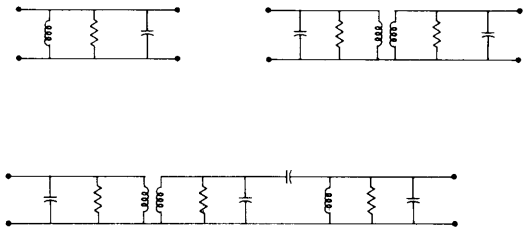

Fig. XVIII-11

Examples of simple-reactance coupled multiple-tuned interstages.

bandpass structures by the conformal transformation

$$\left[\exp\left(\frac{jm\pi}{2}\right)\right]\lambda = s^m\left(s + \frac{1}{s}\right), \text{ where} \tag{17}$$

λ is the lowpass complex frequency variable, suitably normalized; s is the bandpass complex frequency variable, suitably normalized; and m is a rational number such that $-1 < m < 1$. The transformed transfer function can be realized as an i-f amplifier with simple-reactance coupled multiple-tuned interstages (see Fig. XVIII-11). The index m depends on the interstage used. For single-tuned interstages $m = 0$, for double-tuned inductively coupled interstages $m = +1/2$, and for double-tuned capacitively coupled interstages $m = -1/2$. Note that with $m = 0$ the general transformation, Eq. 17, reduces to the well-known transformation

$$\lambda = s + \frac{1}{s} \tag{17a}$$

It is to be noted that the prototypes for Butterworth, Chebyshev, synchronously tuned, and linear-phase characteristics all fall into the class that has no zeros in the finite λ-plane. Thus they can all be realized as i-f amplifiers with various types of interstages. For a critical analysis and details of the design procedure see Chapter III of reference 3.

J. Elkan

References

1. W. E. Thomson, Wireless Engineer (London) 29, No. 349 (1952).
2. L. Storch, Proc. IRE 42, No. 11 (1954).
3. J. Elkan, M. Sc. Thesis, Department of Electrical Engineering, M.I.T. (1955).
4. Tables of Spherical Bessel Functions, Mathematical Tables Project, Nat. Bur. Standards (Columbia University Press, New York, 1947).
5. P. M. Morse, and H. Feshbach, Methods of Theoretical Physics (McGraw-Hill Book Company, Inc., New York, 1953), Table XV, Vol. 2, pp. 1931-33.
6. DeF. L. Trautman, Technical Report No. 41, Electronics Research Laboratory, Stanford University, Stanford, California, Feb. 1, 1952.